Progress In Electromagnetics Research Letters, Vol. 54, 61–66, 2015

Broadband Circularly Polarized Antenna Based on Quarter-Mode Substrate Integrated Cylindrical Cavity Subarray

Zhangjing Wang*, Yahua Ran, Yang Peng, Yang Li, and Yunqing Sun

Abstract—A broadband circularly polarized planar antenna based on a quarter-mode substrate integrated cylindrical cavity subarray is presented in this communication. It is composed of two layers: a quarter-mode substrate integrated cylindrical Cavity (QMSICC) subarray and the feeding network comprised of three Wilkinson power dividers. The measured 10-dB return loss and 3-dB axial ratio bandwidths at the center frequency 5.2 GHz are 40% and 25.5%, respectively. The gain measured for right-hand circular polarization (RHCP) is 4.6 dBi at 5.2 GHz. And it will be used in WLAN operating at 5.2 GHz.

1. INTRODUCTION

Circularly polarized (CP) antennas are widely used in space applications such as satellite communication, maritime wireless communications, and radar system, because they can resolve problems in wireless channels such as polarization mismatch generated by Faraday Effect and interference generated by multi-path effect. Substrate integrated waveguide (SIW) technology, also called laminated waveguide [1] or post-wall waveguide [2], is composed of two rows of conductive cylinders on a printed circuit board (PCB), which has the advantage of easy integration with planar circuits by replacing the conventional microstrip line and strip line [3]. Also it has the merits of low loss, high power capacity, high Q-factor, and low cost than conventional waveguide [4, 5]. Therefore, research into SIW circuits and antennas is gaining lots of interest. SIW-based CP antennas have also been reported by many researchers [6–9]. For instance, in [6], an SIW cavity-backed, crossed-slot antenna is presented. The CP wave is generated in the TE_{12} mode. The CP operation is realized by different lengths of the two arms of the crossed slot to create a 90 phase difference. In [7], a cavity-backed planar slot CP antenna is developed using a half-mode substrate integrated waveguide (HMSIW) technique which the CP radiation is excited by the TE_{120} mode. In [8], a CP SIW antenna is generated in the TE_{220} mode.

However, all the above CP SIW antennas also suffer from narrow AR bandwidth, e.g., 0.8% (10–10.05 GHz) in [6], 1.74% (8.68–8.8 GHz) in [7], 2.8% (10.6–10.9 GHz) in [8]. Therefore, several methods were proposed to improve the AR bandwidth of the SIW-fed antenna array. In [9], it has been improved to 15% (54.5–64 GHz) by placing a rotated strip instead of a dipole above the SIW slot.

In this communication, a quarter-mode substrate integrated cylindrical Cavity (SICC) subarray is proposed for a broadband CP radiation. The reflection coefficient and radiation characteristics of the designed QMSIW subarray antenna are measured, and results show that the antenna exhibits right-handed (RH) CP radiation with a gain of 4.6 dB and a wide 3 dB axial ratio (AR) bandwidth of 25.7% around 5.2 GHz.

Received 24 May 2015, Accepted 25 June 2015, Scheduled 15 July 2015
* Corresponding author: Zhangjing Wang (zjwang@uestc.edu.cn).
The authors are with the University of Electronic Science and Technology of China, Chengdu 610054, China.

2. ANALYSIS AND ANTENNA DESIGN

2.1. SICC and QMSICC Antenna

Substrate Integrated Cylindrical Cavity (SICC) is a cylindrical cavity with side wall of metallic vias instead of solid metallic sidewall connecting the solid metallic top and bottom plates, as shown in Figure 1(a). R is the radius of Substrate Integrated Cylindrical Cavity, r the via hole radius, s the spacing between adjacent via holes, d_1 the radius of the feed probe, and d_2 the spacing between the center of the via holes and the edge of the patch. The equivalent radius of the circular cavity and restrictions are [10]

$$R_{eq} = \sqrt{(R+r)\cdot(R-r)}\cdot\left[\frac{\pi}{n\ln\dfrac{R+r}{R-r}}\right]^{\frac{\pi}{2n}} \tag{1}$$

$$\begin{cases}\dfrac{\pi}{n} \le \ln\left(\dfrac{R+r}{R-r}\right) \le \dfrac{\lambda_{\min}}{10} \\ \dfrac{\pi R}{2n} \le r \le \dfrac{\lambda_{\min}}{20}\end{cases} \tag{2}$$

where n is the number of metallic vias and $\lambda_{\min}$ the minimum wavelength corresponding to the maximum operation frequency.

The resonant frequencies of TM and TE modes of the Substrate integrated waveguide cylindrical cavity can be expressed by [11]

$$\begin{aligned}(f_r)_{npq}^{TM} &= \frac{1}{2\pi R_{eq}\sqrt{\varepsilon\mu}}\sqrt{x_{np}^2+\left(\frac{q\pi R_{eq}}{h_1}\right)^2} \\ (f_r)_{npq}^{TE} &= \frac{1}{2\pi R_{eq}\sqrt{\varepsilon\mu}}\sqrt{x_{np}'^2+\left(\frac{q\pi R_{eq}}{h_1}\right)^2}\end{aligned} \tag{3}$$

where $n = 0, 1, 2, \ldots$; $p = 1, 2, \ldots$; $q = 0, 1, 2 \ldots$; h_1 is thickness of the substrate. Each n except $n = 0$ denotes a pair of degenerate modes ($\cos n\phi$ or $\sin n\phi$ variation). x_{np}, x'_{np} are the zeros of $J_n(x)$ and $J'_n(x)$, respectively. For $h_1/R_{eq} < 2$, the TM_{010} mode is the dominant mode of the substrate integrated waveguide cylindrical cavity, and the resonant frequency is

$$f_0 = \frac{c}{2.62R_{eq}\sqrt{\varepsilon_r}} \tag{4}$$

where, C is the light velocity in air and ε_r the relative permittivity of dielectric substrate.

Given the symmetry of the electric field distribution in the cavity, the symmetry plane behaves as a virtual magnetic wall. Therefore, as described in Figure 1(b), the cavity is split along $x = 0$ and $y = 0$,

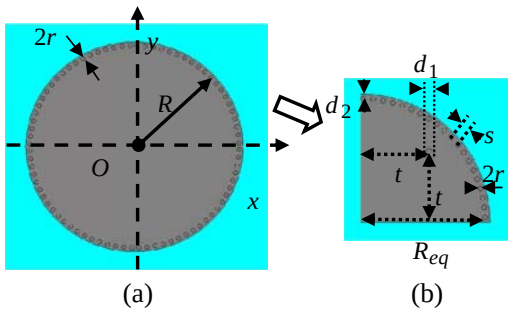

Figure 1. (a) Geometry of the substrate integrated cylindrical cavity. (b) Configuration of the quarter-mode substrate integrated cylindrical cavity linearly polarized antenna.

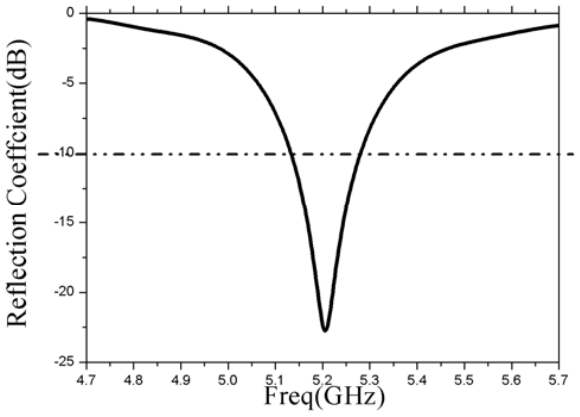

Figure 2. Simulated reflection coefficient of the quarter-mode substrate integrated waveguide linearly polarized antenna.

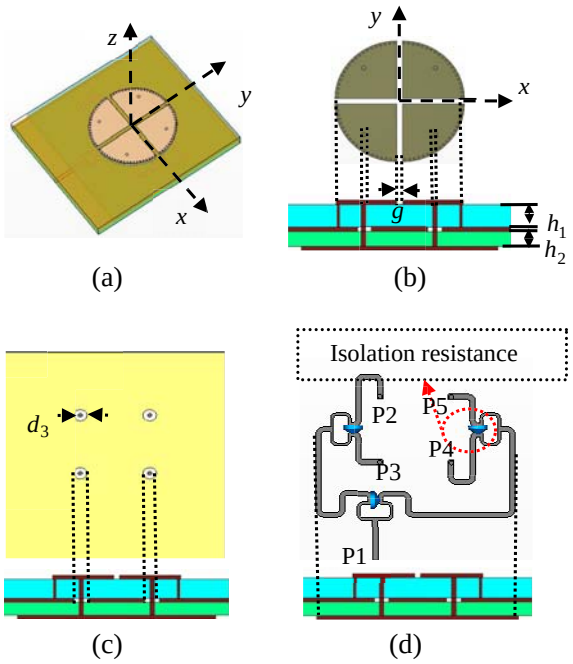

Figure 3. Top view of the QMSICC circularly polarized antenna. (a) Three dimensional model. (b) Radiator on the top layer. (c) Ground plane layer. (d) Power distribution network on the bottom layer.

leading to a size reduction of almost 75% without significant change of the resonant frequency [12, 13]. Therefore, we can use Equations (1), (2) and (4) to design substrate integrated waveguide cylindrical cavity and QMSICC accurately.

Based on the qualitative analysis of the SICC and QMSICC, a simple linearly polarized antenna is designed and shown in Figure 1(b). The antenna uses Teflon substrate with thickness h_1, low dielectric constant ($\varepsilon_r = 2.65$) and low loss tangent ($\tan\delta < 0.0002$). Figure 2 shows simulated reflection coefficient of the linearly polarized antenna based on the QMSICC. The first resonance occurs at 5.2 GHz, corresponding to the TM_{010} mode of the QMSICC.

In order to achieve a CP antenna, four linearly polarized QMSICC antennas of the same dimensions are symmetrically located with respect to the center of the square substrate and are fed in phase rotation by Wilkinson power divider.

2.2. Antenna Design

Figure 3 shows the geometrical configuration for the antenna with top view. It is composed of two layers: a quarter-mode substrate integrated cylindrical Cavity (QMSICC) subarray and the matching network. The QMSICC subarray, which uses Teflon ($\varepsilon_r = 2.65$) and low loss tangent ($\tan\delta < 0.0002$), is achieved by sequential rotation of the QMSICC antenna. The four QMSICC antennas of the same dimensions as the QMSIW linearly polarized antenna shown in Figure 1(b) are symmetrically located with respect to the center of the square substrate and are fed by probe of diameter d_1 in phase rotation to achieve circular polarization. The bottom layer is a feed network made by three Wilkinson power dividers, of which the feeding lines are printed on a square Rogers RO 4350B substrate with a dielectric constant of 3.48, height of 0.508 mm, and low loss tangent 0.0022. The widths of the $50, 70.7\,\Omega$ microstrip lines are 1.16 mm and 0.63 mm, respectively.

Figure 4 shows the simulated transmission characteristics of the feed network. From 4.4 to 6 GHz, the power imbalance between feed ports was within ± 0.4 dB, although extra insertion losses were

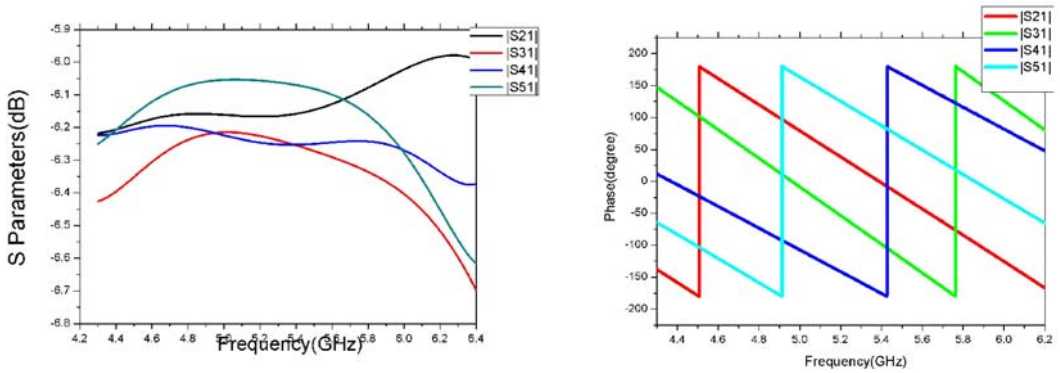

(a) (b)

Figure 4. Simulated transmission characteristics of designed feed network. (a) Magnitude response. (b) Phase response.

observed at frequencies below 4.4 GHz and beyond 6 GHz, as shown in Figure 4(a). Ideally, feed ports P2 to P5 have progressive phases from 0° to 270° insteps of 90°. However, the simulated results indicate a phase error of ±15° for a bandwidth of 4.4 to 6 GHz, as shown in Figure 4(b). Four ports (P2, P3, P4, P5) with almost identical magnitude and 90-degree phase difference between adjacent elements at the center frequency of 5.2 GHz are designed to feed each QMSICC element by four pins as shown in Figure 3(d). By sweeping the parameters and optimizing the structure, the final size of the antenna is obtained: $d_1 = 0.92$ mm, $d_2 = 0.5$ mm, $d_3 = 3.18$ mm, $s = 1$ mm, $t = 6.975$ mm, $g = 1.2$ mm, $r = 0.25$ mm, $R = 13.1$ mm, $h_1 = 1.5$ mm, $h_2 = 0.508$ mm.

3. SIMULATIONS AND MEASURED RESULTS

The proposed antenna is designed with CST Microwave Studio based on a finite-difference time-domain algorithm [14]. Figure 5 shows the fabricated prototype of the designed CP antenna with the same dimensions indicated in Figure 3. The simulated and measured return losses are shown in Figure 6 with the vector network analyzer E8363B from Agilent Technologies. The difference between simulated and measured results in Figure 6 is attributed to the material and manufacturing tolerance and a multilayer implementation. It can be seen from Figure 6 that the measured 10-dB return loss bandwidth is 40% (3.9 GHz–6.25 GHz) at the center frequency 5.2 GHz.

Figure 7 shows the measured and simulated peak gains of the proposed CP antenna. The measured maximum gain is 4.59 dBi, while the simulated one is 5.23 dBi at 5.2 GHz. The simulated and measured AR results are plotted in Figure 7. The measured radiation efficiency is 70.7%, while the simulated one is 79.3% at 5.2 GHz. The decrease in the measured gain and radiation efficiency might be due to mismatch of the feeding network and dielectric loss. The simulated and measured AR results are also plotted in Figure 7. The measured AR of the antenna is around 0.29 dB at 5.2 GHz, and the measured

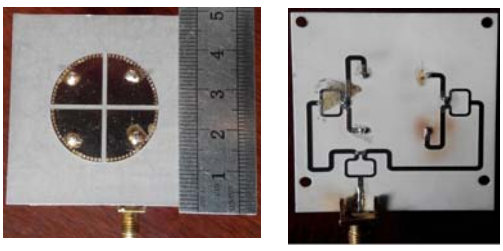

(a) (b)

Figure 5. Prototype of the circularly polarized antenna. (a) Radiator on the top layer. (b) Matching network on the bottom layer.

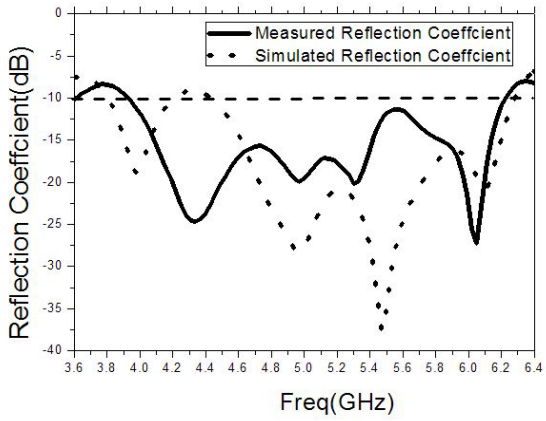

Figure 6. Reflection coefficients and radiation efficiency of the proposed circularly polarized antenna.

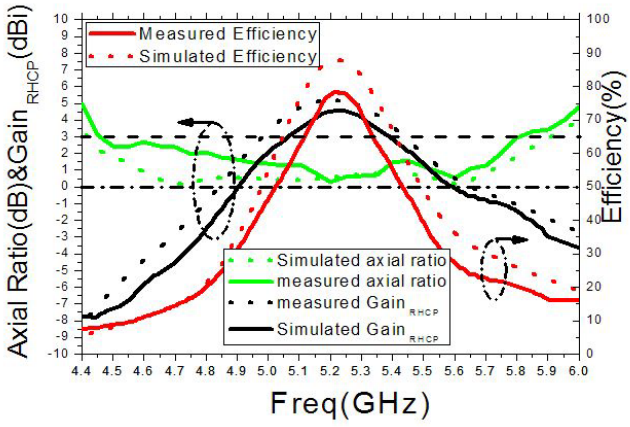

Figure 7. Simulated and measured gain, axial ratio and radiation efficiency of the proposed circularly polarized antenna.

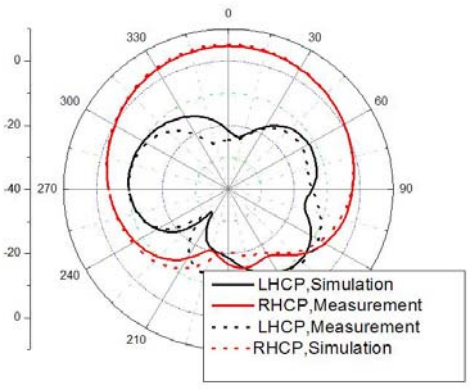

(a) *x*-*z* cut plane

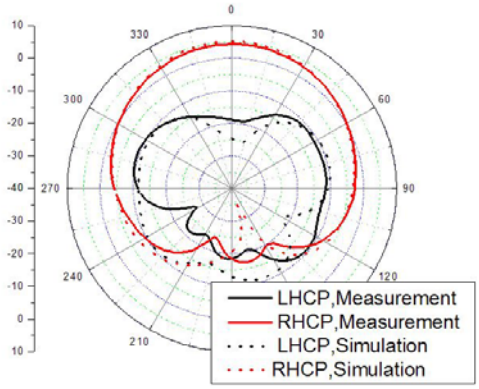

(b) *y*-*z* cut plane.

Figure 8. Simulated and measured radiation patterns of the QMSICC circularly polarized antenna at 5.2 GHz. (a) *x*-*z* plane. (b) *x*-*y* plane.

3 dB AR bandwidth is 25.7% from 4.47 GHz to 5.81 GHz, respectively.

The radiation patterns are simulated and measured to demonstrate the radiation characteristics of the proposed QMSICC subarray antenna. The simulated and measured radiation patterns of the proposed antenna at 5.2 GHz are shown in Figure 8. From Figure 8, it is seen that antenna is a right-hand circularly polarized (RHCP) antenna. A good CP radiation beam is generated by this QMSIW subarray, and the main lobe points to the broadside direction.

4. CONCLUSION

This letter presents a QMSICC subarray for circular polarization. The proposed planar CP antenna has been simulated, fabricated and tested, and its radiation characteristics have been demonstrated. The measured 10-dB return loss and 3-dB axial ratio bandwidths at the center frequency 5.2 GHz are 40% and 25.5%, respectively. The gain measured for right-hand circular polarization (RHCP) is 4.6 dBi at 5.2 GHz. And the proposed antenna still retains many advantages such as low profile, light weight, low fabrication cost, and easy integration with planar circuits. And it will be used in WLAN operating at 5.2 GHz.

REFERENCES

1. Uchimura, H., T. Takenoshita, and M. Fujii, "Development of a 'laminated waveguide'," *IEEE Trans. Microw. Theory Tech.*, Vol. 46, No. 12, 2438–2443, Dec. 1998.
2. Hirokawa, J. and M. Ando, "Efficiency of 76-GHz post-wall waveguide-fed parallel-plate slot arrays," *IEEE Transactions on Antennas and Propagation*, Vol. 48, No. 11, 1742–1745, Nov. 2000.
3. Deslandes, D. and K. Wu, "Accurate modeling, wave mechanisms, and design considerations of a substrate integrated waveguide," *IEEE Trans. Microw. Theory Tech.*, Vol. 54, No. 6, 2516–2526, Jun. 2006.
4. Cassivi, Y., L. Perreprini, P. Arcioni, et al., "Dispersion characteristics of subsrtate integrated rectangular waveguide," *IEEE Microw. Wireless Compon. Lett.*, Vol. 12, No. 9, 333–335, 2002.
5. Xu, F. and K. Wu, "Guided-wave and leakage characteristics of substrate integrated waveguide," *IEEE Trans. Microw. Theory Tech.*, Vol. 53, No. 1, 66–73, 2005.
6. Luo, G. Q., Z. F. Hu, Y. Liang, L. Y. Yu, and L. L. Sun, "Development of low profile cavity backed crossed slot antennas for planar integration," *IEEE Transactions on Antennas and Propagation*, Vol. 57, No. 10, 2972–2979, Oct. 2009.
7. Razavi, S. and M. Neshati, "Development of a low profile circularly polarized cavity backed antenna using HMSIW technique," *IEEE Transactions on Antennas and Propagation*, Vol. 61, No. 3, 1041–1047, 2013.
8. Jin, C., R. Li, A. Alphones, and X. Bao, "Quarter-mode substrate integrated waveguide and its application to antennas design," *IEEE Transactions on Antennas and Propagation*, Vol. 61, No. 6, 2921–2928, Jun. 2013.
9. Li, Y., et al., "Axial ratio bandwidth enhancement of 60-GHz substrate integrated waveguide-fed circular polarized LTCC antenna array," *IEEE Transactions on Antennas and Propagation*, Vol. 60, No. 10, 4619–4626, Oct. 2012.
10. Luan, X.-Z. and K.-J. Tan, "Equivalent radius analytic formulas of substrate integrated cylindrical cavity," *Proc. Antenna & Propagation (ISAP)*, 746–749, 2013.
11. Harrington, R. F., *Time-harmonic Electromagnetic Fields*, 2nd Edition, Chapter 5.4, Wiley-IEEE, 2001.
12. Sam, S. and S. Lim, "Electrically small eighth-mode substrate-integrated waveguide antenna with different resonant frequencies depending on rotation of complementary split ring resonator," *IEEE Transactions on Antennas and Propagation*, Vol. 61, No. 10, 4933–4939, 2013.
13. Kang, H. and S. Lim, "Electrically small dual-band reconfigurable complementary split-ring resonator (CSRR)-loaded eighth-mode substrate integrated waveguide (EMSIW) antenna," *IEEE Transactions on Antennas and Propagation*, Vol. 62, No. 5, 2368–2373, 2014.
14. CST Microwave Studio (MWS) CST Corporation, Online Available: http://www.cst.com, 2008.